

The influence of two-dimensional roughness element on boundary flow structure in the favorable pressure gradient region of the swept wing

Stepan Tolkachev, Victor Kozlov* and Valeriya Kaprilevskaya**

**Khristianovich Institute of Theoretical and Applied Mechanics SB RAS*

Novosibirsk, Russia, 630090

Abstract

In this article presented the results of research of development of stationary and secondary disturbances behind the localized and two-dimensional roughness elements. It is shown that the two-dimensional roughness has a destabilizing effect on the disturbances induced by the three-dimensional roughness element, which lies upstream. In this case, the two-dimensional roughness can lead to the appearance of stationary structures, and then secondary perturbations, whose frequency range lies lower than in the case of the excitation of stationary vortices by a three-dimensional roughness.

1. Introduction

Flights at transonic speeds require the use of swept wings on aircraft. However, this wing, in comparison with the straight one, has an additional instability mechanism due to the presence of a secondary flow, which leads to a laminar-turbulent transition in the region of a favorable pressure gradient.

Modern aircraft manufacturers are intensively developing a laminarized aircraft, which in the future can provide a 15% reduction in fuel consumption. However, in this way there are a lot of problems, since even micron-sized roughnesses can cause a localized area of laminar-turbulent transition in the transverse direction so the line of transition becomes a jagged.

The laminar-turbulent transition mechanism caused by roughness was studied in [1 - 2], [3]. In [1 - 2], investigations were carried out in the region of the neutral pressure gradient. It is shown that the edge of the roughness element causes the appearance of a single vortex (longitudinal structure), which leads to the appearance of two modes of secondary disturbances, which ultimately leads to laminar-turbulent transition [1]. It was shown that in the interacting two counterrotating vortices, the stability of the boundary layer can be higher [2] than in the case of isolated vortices. The appearance of additional stationary vortices as a result of the nonlinear development of secondary perturbations is revealed. In [3], studies were carried out using regular micron roughnesses. Depending on the interval between the roughness elements, one of the two high-frequency modes (transverse and normal) predominated [3]. However, the question remained about the troubles in those experiments with the excitation the mode of secondary perturbations by the acoustics.

It was shown in [4] that the laminar-turbulent transition scenario depends on the freestream velocity. Secondary disturbances under natural conditions have the form of a wave packet. At low flow speed, the non-linear development scenario occurs with the filling of the low-frequency component of the spectrum. An increase in the speed of the oncoming stream leads to an increase in the amplitude of the wave packet to 1% of the freestream velocity. After this stage harmonics of the wave packet appear with subsequent filling of the spectrum to the turbulent state.

The design of the modern wing with its mechanization is very complicated, thus two-dimensional and three-dimensional roughness can be highlighted. The most revealing example of a two-dimensional roughness is the joint of the slat. Examples of three-dimensional roughness are natural surface roughness, rivets, vortex generators, insects, snow, etc.

The emphasis is placed on the study of a two-dimensional roughness separately, as well as its influence on the development of a stationary vortex, excited by a cylindrical roughness.

2. Experimental techniques

2.1. Measurement conditions

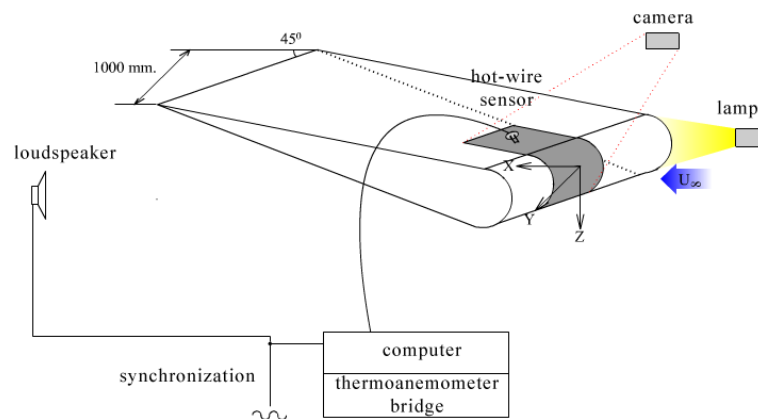


Figure 1: Scheme of experiment.

The experiment was carried out in the test section of a low-turbulent wind tunnel AT-324, the dimensions of which are $1000 \times 1000 \times 4000$ mm. The freestream velocity was controlled by a Pitot-Prandtl nozzle connected to an electronic manometer and was set to $V_\infty = 10.9$ m/s. The air temperature was 296° K.

The noise level of the working wind tunnel was measured with a soundproofing device with a windproof attachment in the pre-chamber before the confuser behind the pivoting blades before the deturbulising nets (50.7 dBA) and after the deturbulising nets (47.9 dBA). The degree of flow compression in the installation was 17.5, so the flow velocity in the noise measurement was about 0.68 m/s. In this case, according to the instructions, when using a windproof hood, it is allowed to measure the noise level at wind speeds up to 5 m/s.

2.2. The wing model

For the studies, a sliding-wing model was chosen whose profile is formed by a cylinder of radius $r = 40$ mm and two converging planes. The chord of the wing is $Ch = 400$ mm. The slip angle is $\chi = 45^\circ$.

The angle of attack was chosen to realize a favorable pressure gradient over the flat part of the wing profile and was $\alpha = -12.3^\circ$. On the wing model, end plates were installed to cut off disturbances that develop on the walls of the test section. At the downside of the wing model, turbulizers are installed to prevent flow separation.

2.3. The liquid crystal thermography

An investigation of the flow structure near the wall was carried out by the liquid-crystal thermography technique, which was described in detail in [5, 6]. At the same time, the liquid crystal film was heated to a working temperature range between the 303° K and 306° K. To represent the results of visualization, it was decided to present the data in color coordinates.

2.4. Hot-wire anemometry measurements

As a measuring technique, the hot-wire anemometry of constant temperature was chosen.

Before the measurements, the sensor wire of the anemometer was installed parallel to the surface of the swept-wing model and perpendicular to the freestream direction.

The calibration of the sensor was carried near the Pito-Prandtl nozzle in the speed range from 0 to 16 m/s.

2.5. Stationary disturbances excitation

Excitation of stationary disturbances was carried out by a three-dimensional cylindrical roughness of 0.8 mm in height and 1.6 mm in diameter.

In experiments using liquid-crystal thermography with orientation to work [4], performed earlier on this wing model, the cylindrical roughness was located at 64.2° from the line of symmetry of the wing profile to realize the effective excitation of stationary and secondary perturbations. The effect of a two-dimensional roughness 0.13 mm thick, 15 mm wide and 200 mm long was also investigated. The height of the two-dimensional roughness could vary from 0 to 1.6 mm due to a set of such roughness elements.

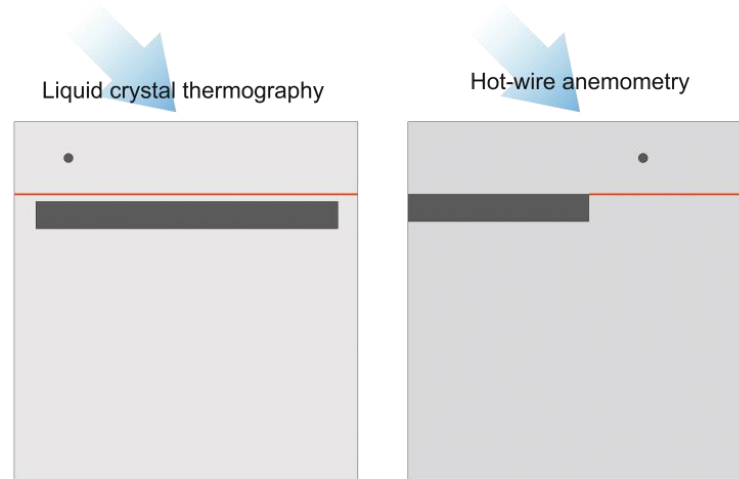


Figure 2: The locations of two-dimensional and cylindrical roughness on the wing model. The red line shows the line of transition of the cylindrical profile part to the flat one.

For hot-wire measurements, a two-dimensional roughness of 15 mm wide, 118 mm long, 0.91 mm high was chosen. The cylindrical roughness was placed at 63.1° from the line of symmetry of the wing profile.

2.6. Secondary disturbances excitation

The excitation of secondary disturbances was carried out by the loudspeaker connected to the sound generator.

In the first series of experiments, the technique of liquid-crystal thermography did not allow quantitative comparison of the acoustic effect on the mean flow. Studies were carried out in the frequency range from 100 Hz to 3000 Hz in steps of 100 Hz. For the presentation of the results, it was chosen the modes 500 Hz and 1800 Hz.

In the second series of experiments, hot-wire measurements behind the two-dimensional roughness element showed that the natural disturbances have the form of a wave packet with a maximum near 700 Hz, so this frequency was chosen for further studies of the development of secondary perturbations.

Preliminary hot-wire measurements made it possible to choose two modes of acoustic excitation regimes with different amplitudes. Measurements with a sound level meter in the wind tunnel test section without a flow showed: a mode of small acoustic influence 50.1 dB, a loud acoustic regime is 65 DBA at a frequency of 700 Hz.

2.7. The coordinate system

The following coordinate system is used in this paper:

- The X axis is directed along the stream;
- The Y axis is perpendicular to the X axis. Note that the axis of the cylindrical part of the wing profile lying in the XY plane;
- The Z axis is perpendicular to the X and Y axes;
- The Xw axis is parallel to the X axis, but has a value of 0 above the line of transition of the cylindrical profile part to the flat one.

Thus, the Xw-Y coordinate system is oblique, which facilitates the interpretation of data in the investigation of the swept wing.

3. The measurement results

3.1. The liquid crystal thermography

After setting the angle of attack, it was necessary to make sure that a favorable pressure gradient is realized above the wing. For this purpose, hot-wire measurements were performed on the wing model at a distance of 20 mm from the surface (Figure 3).

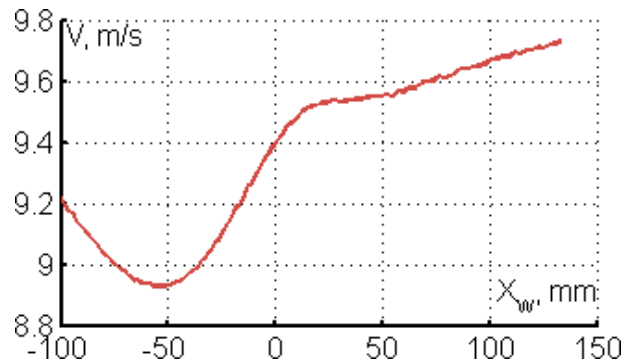


Figure 3: Velocity distribution above the wing model on 20 mm from the surface.

On the flat part of the wing model, a two-dimensional roughness was placed in layers of 0.13 mm in thickness. In Figure 4, the results of visualization by the liquid-crystal thermography method for various thicknesses of the two-dimensional roughness h_{2d} are presented.

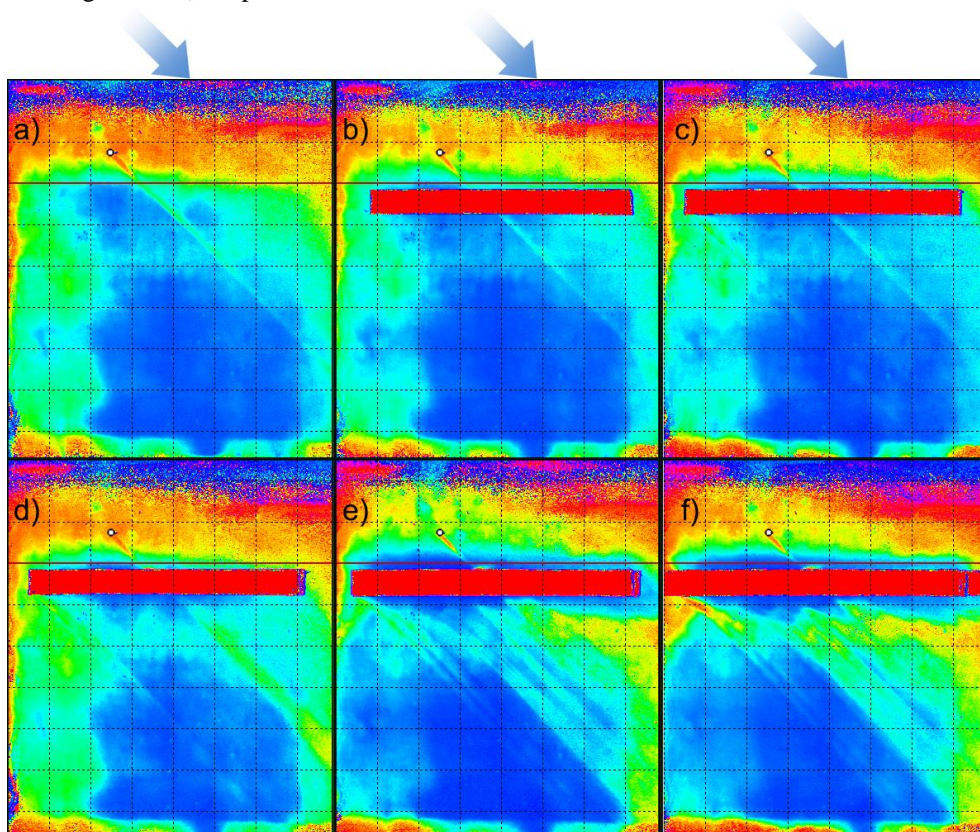


Figure 4: The effect of the height of the two-dimensional roughness h_{2d} on the trace behind the cylindrical roughness element: a) $h_{2d} = 0$ mm; b) $h_{2d} = 0.26$ mm; c) $h_{2d} = 0.52$ mm; d) $h_{2d} = 0.78$ mm; e) $h_{2d} = 1.56$ mm; f) $h_{2d} = 1.82$ mm.

Behind the cylindrical roughness a pair of counterrotating vortices is formed, one of which dies very quickly, and the amplitude of the second one reaches its saturation (Figure 4a). The bonding of a two-dimensional roughness to a height of 0.26 mm on the visualization does not lead to a visible change of the flow structure (Figure 4b). A further increase of the height of the two-dimensional roughness element leads to the appearance of additional

stationary vortices (Figure 4c), amplification of pulsations (Figure 4d), and turbulence of the flow in the wake behind the cylindrical roughness (Figure 4e, Figure 4f).

It is noticed that longitudinal structures are formed behind a two-dimensional roughness with a height of more than 0.91 mm (Figure 5b). At the same time, the wavelength changed with the change in the height of the two-dimensional roughness (Figure 5b, Figure 5c).

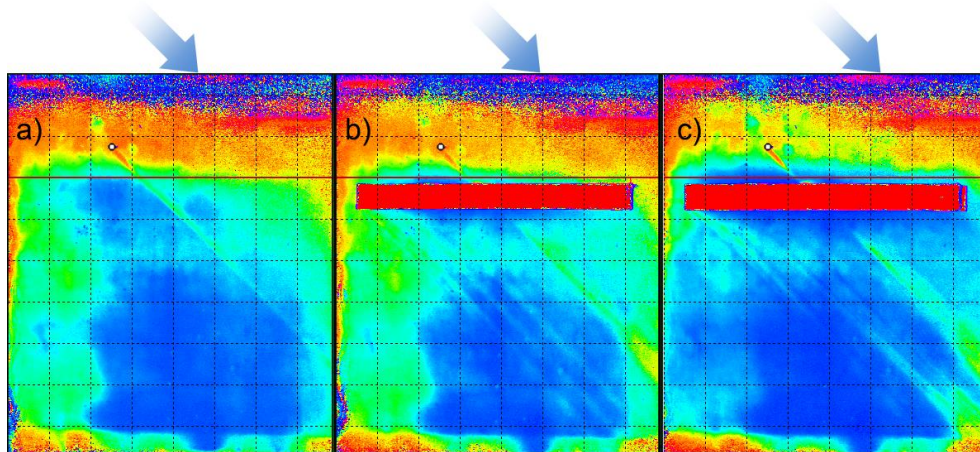


Figure 5: The influence of the height of the two-dimensional roughness h_{2d} on the development of stationary structures: a) $h_{2d} = 0$ mm; b) $h_{2d} = 0.91$ mm; c) $h_{2d} = 1.3$ mm.

The next step was to investigate the excitation of secondary disturbances by acoustics. Cylindrical roughness element excites stationary vortices, leading to the appearance of a packet of secondary disturbances at frequencies of about 1800 Hz (Figure 6c). Even the interaction with the two-dimensional roughness of the prevailing increasing frequency does not change (Figure 6e). However, stationary vortices excited by a two-dimensional roughness lead to the appearance of a packet of secondary disturbances at lower frequencies of about 500 Hz (Figure 6d). This phenomena can be connected with a different structure of stationary vortices.

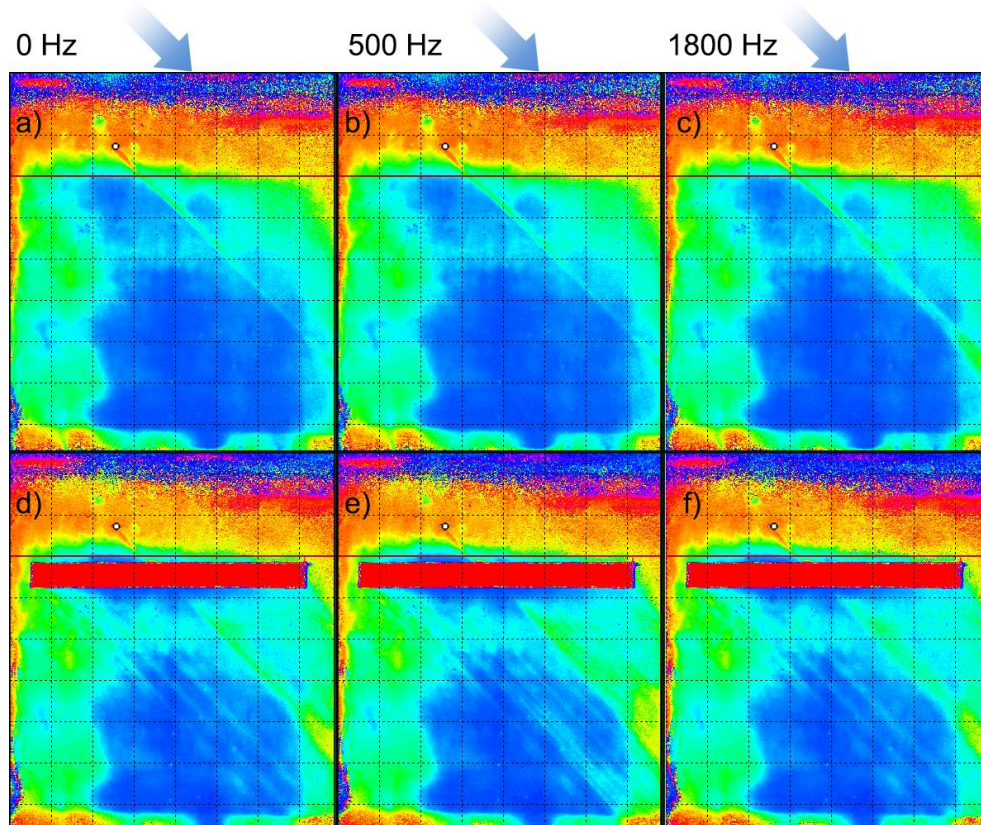


Figure 6: Excitation of secondary disturbances by an acoustic field of frequency f ($f = 0$ Hz for a, d; $f = 500$ Hz for b, e; $f = 1800$ Hz for c, f) for excitation of stationary disturbances only by cylindrical roughness element (a, b, c) and the case of interacting with a two-dimensional roughness $h_{2d} = 0.91$ mm (d, e, f).

3.2. Hot-wire anemometry measurements

Hot-wire anemometry made it possible to investigate flow over a two-dimensional roughness (Figure 7). It can be seen from the results that the longitudinal structures begin to form at the leading edge of the step. The transverse scale of these disturbances is $\lambda_Y = 4 - 8$ mm. The injection of acoustic disturbances at a frequency of 700 Hz leads to the appearance of a signal amplitude up to 0.015%. And the maximum values are reached near inflection points in the transversal velocity distribution.

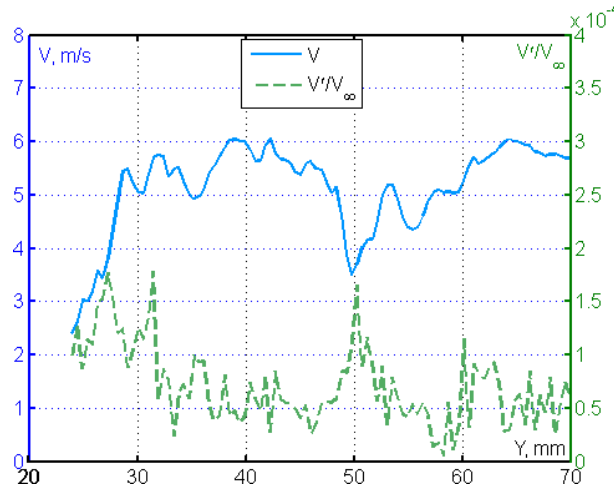


Figure 7: Distribution of the mean velocity and amplitude of the excited mode at a frequency of 700 Hz over a two-dimensional roughness.

The distribution of the mean velocity behind the roughness element at distances $X_W = 36.7$ mm, $X_W = 60.9$ mm, $X_W = 133.5$ mm is shown in Figure 8. The transverse scale of the longitudinal structures is $\lambda_Y = 4 - 5$ mm, which connects with the scale of disturbances at the leading edge of the two-dimensional roughness. The amplitude of longitudinal disturbances decreases along the stream. In this case, perturbations created by the ends of a two-dimensional roughness, as well as a three-dimensional cylindrical roughness, were not taken into consideration.

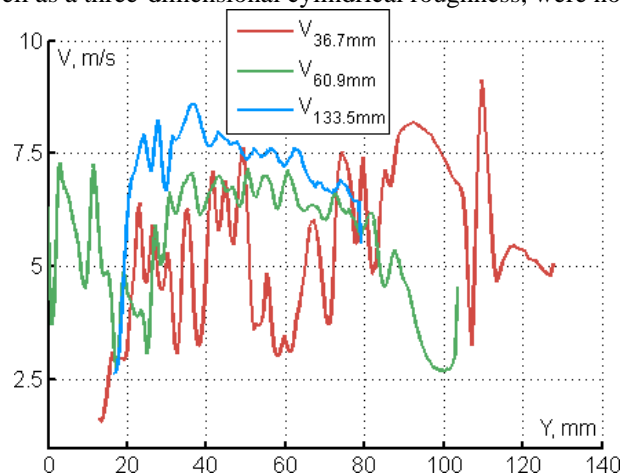


Figure 8: The velocity distribution behind the two-dimensional and three-dimensional roughness at distances $X_W = 36.7$ mm, $X_W = 60.9$ mm, $X_W = 133.5$ mm.

A more detailed investigation of longitudinal vortices and secondary instability on them was carried out in an area in which the ends of the two-dimensional roughness had no effect. In Figure 9 the distribution of the time-averaged velocity and the amplitude of the disturbance at a frequency of 700 Hz is presented for the cases of excitation by acoustics with different volume levels at the position $X_W = 39$ mm. The graph shows that the secondary perturbations are excited near inflection points in the transversal distribution of the mean velocity. In order to be able to compare the behavior of the amplitude distribution in the space for these regimes, the amplitude of the perturbation, which is excited by large amplitude acoustics, is reduced by a factor of 10.

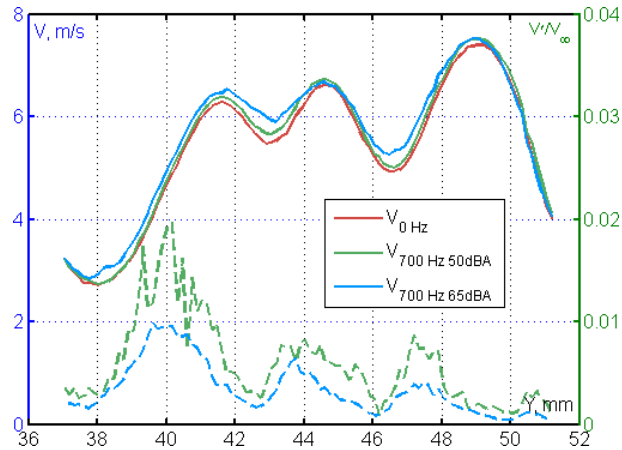


Figure 9: The distribution of the time-averaged speed (solid lines) and the amplitude of the 700 Hz mode (dashed lines) behind the two-dimensional roughness at a distance of $X_w = 39$ mm (the amplitude of the 700 Hz mode for loud mode is reduced by a factor of 10).

At a point near one of the maximums $Y = 47.2$ mm, the spectrum of velocity pulsations is presented (Figure 10). It is seen that there is a wave packet lying in the frequency range 400 - 900 Hz. Acoustic field leads to excitation of the isolated mode, but does not lead to a change in the other part of velocity spectrum. The excitation of a large amplitude by acoustics leads to the appearance of a second harmonic of the secondary perturbation.

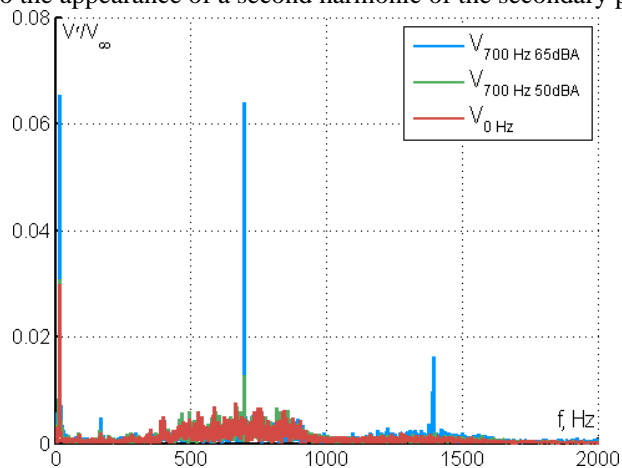


Figure 10: The pulsation spectra at the point $X_w = 39$ mm, $Y = 47.2$ mm.

At the position $X_w = 94$ mm, the character of the velocity distribution is smoothed in comparison with $X_w = 39$ mm (Figure 11). The distribution of the amplitude of the 700 Hz mode is rather noisy, the maxima are less pronounced, the amplitude of the mode of the secondary perturbation is smaller.

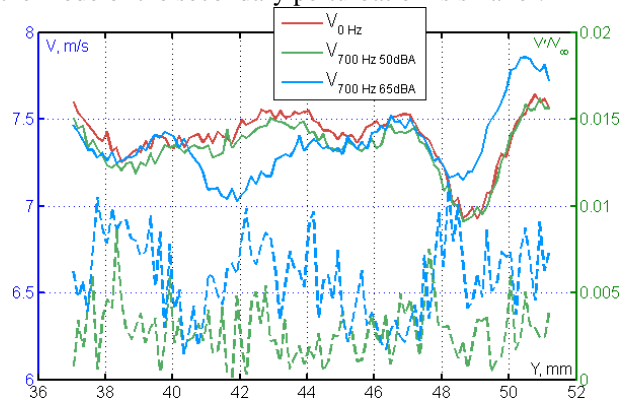


Figure 11: The distribution of the time-averaged velocity (solid lines) and the amplitude of the 700 Hz mode (dashed lines) behind the two-dimensional roughness at a distance of $X_w = 94$ mm.

The velocity spectrum at the point $Y = 47.9$ mm is turbulent (Figure 12). In this case, a disturbance with a frequency of 700 Hz is not highlighted on the spectrum.

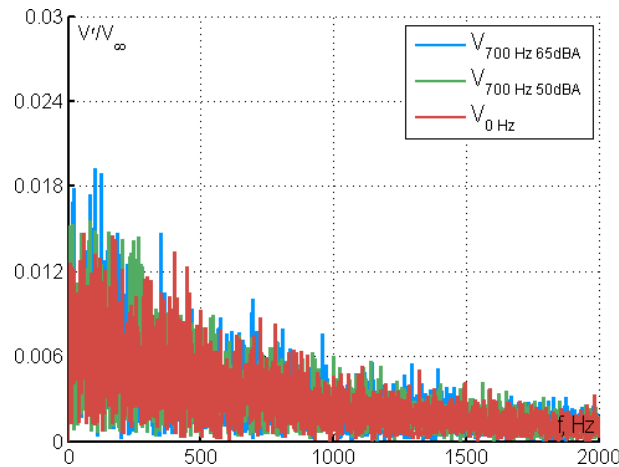


Figure 12: The pulsation spectra at the point $X_w = 94$ mm, $Y = 47.9$ mm.

Secondary disturbances were investigated using the technique of controlled perturbations. To simplify the hot-wire measurements, it was decided to carry out measurements along the trajectory along the X_w axis at a fixed Y . Because the mode under investigation turned out to be "hard" (a sufficiently high velocity of the incoming flow combined with a large height of the two-dimensional roughness), an increase in the mode amplitude of 700 Hz occurs only 3 mm along the path, and then the amplitude decreases (Figure 13).

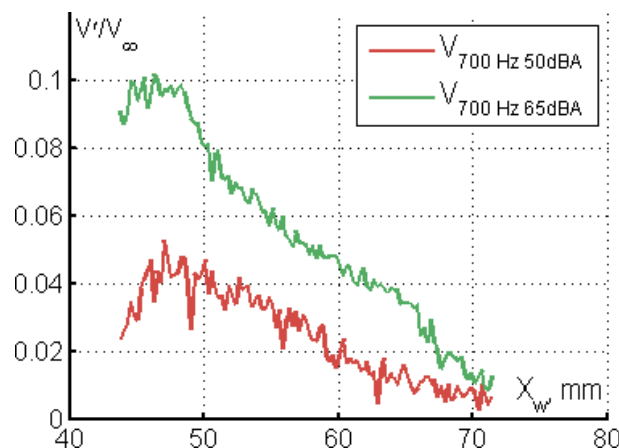


Figure 13: Change of the disturbance amplitude of the 700 Hz mode disturbance at $Y = 49.2$ mm along the X_w direction.

Measurements of phase along the trajectory (Figure 14) showed that we are dealing with traveling secondary disturbances whose wavelength is much less than acoustic perturbations.

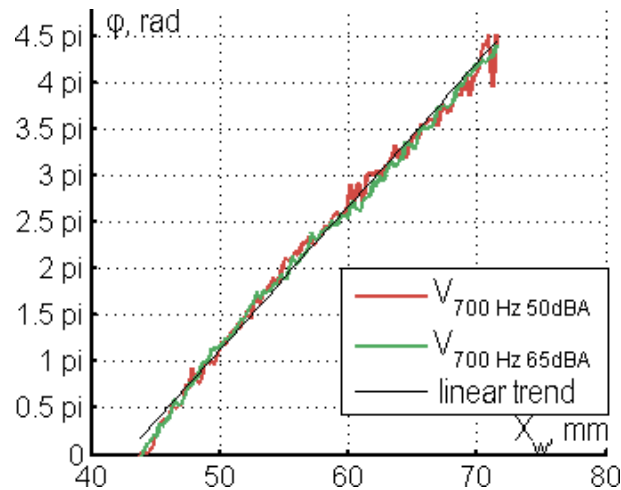


Figure 14: Change of the disturbance phase of the 700 Hz mode disturbance at $Y = 49.2$ mm along the X_w direction.

4. The discussion of the results

An interesting result is the excitation of three-dimensional longitudinal structures by the two-dimensional roughness element. The presence of a transverse flow makes the boundary layer receptive to localized inhomogeneities in the transversal velocity distribution, arising from the nonideality of the surface of the two-dimensional roughness. The mechanism of selection by wavelengths distinguishes the most unstable.

The second interesting fact is related to the difference in the frequencies of the secondary disturbances excited by the cylindrical and two-dimensional roughness elements.

5. Conclusions

A destabilizing effect of two-dimensional roughness on the development of perturbations behind the three-dimensional roughness element was found in the work. In addition, in itself, the two-dimensional roughness leads to the appearance of stationary vortices. However, the frequencies of increasing secondary perturbations in stationary vortices generated by three-dimensional and two-dimensional roughness elements differ from each other.

Hot-wire measurements have shown that longitudinal structures are generated on the front step of a two-dimensional roughness. Above the two-dimensional roughness in the region of inflection points in the transversal velocity distribution, secondary disturbances are generated. The back step leads to the appearance of a local separation, which contributes to a sharp increase in disturbances.

The development of secondary disturbances downstream could contain the mechanism of the appearance of multiple harmonics if the amplitude becomes sufficiently high (more than 1.5% of the freestream velocity). Eventually, the flow becomes turbulent, which leads to a decrease in the amplitude of the stationary perturbation.

6. Acknowledgments

We thank Valentina Kovrizhina and Galina Zharkova for their help in adaptation liquid crystal thermography for this experiment. This work was partially funded by the grant of the President of the Russian Federation Scientific School (NSH-8788.2016.1) and RFBR Grant 15-08-01945.

References

- [1] A. V. Boiko, V. V. Kozlov, V. V. Syzrantsev, V. A. Shcherbakov Experimental study of the transition to turbulence at a single stationary disturbance in the boundary layer of an oblique aerofoil, *Journal of Applied Mechanics and Technical Physics* (1995) Vol. 36, Issue 1, pp. 67–77.
- [2] Chernoray V. G., Dovgal A. V., Kozlov V. V., Lofdahl L. Secondary Instability of a Swept-Wing Boundary Layer Disturbed by Controlled Roughness Elements, *Journal of Visualization* (2010) Vol. 13. pp. 251–256.

- [3] White E. B., Saric W. S. Secondary Instability of Crossflow Vortices, *J. Fluid Mech.* (2005) Vol. 525. pp. 275–308.
- [4] S. N. Tolkachev, V. N. Gorev, V. V. Kozlov Investigation of formation and development of stationary and secondary disturbances in the favourable pressure gradient area on the swept wing, *Vestnik NSU. Series: Physics* (2013) Vol. 8, Issue 2. pp. 55-69.
- [5] S. N. Tolkachev, V. N. Gorev, G. M. Zharkova, V. N. Kovrizhina Experimental techniques of the study of the vortex disturbances structure caused by point injection on the swept wing leading edge, *Vestnik NSU. Series: Physics* (2012) Vol. 7, Issue 2. pp. 66-79.
- [6] A. P. Brylyakov, G. M. Zharkova, B. Yu. Zanin, V. N. Kovrizhina, D. S. Sboev. Effect of Free-Stream Turbulence on the Flow Structure near a Wedge and the Windward Side of an Airfoil, *Journal of Applied Mechanics and Technical Physics* (2004) Vol. 45, Issue 4, pp. 510–516.